Plant Physiol. (1992) 99, 203–212
0032-0889/92/99/0203/10/$01.00/0

Received for publication June 26, 1991
Accepted December 9, 1991

Structural Changes and Associated Reduction of Hydraulic Conductance in Roots of *Sorghum bicolor* L. following Exposure to Water Deficit[1]

Rolando T. Cruz, Wayne R. Jordan, and Malcolm C. Drew*

Departments of Soil and Crop Sciences (R.T.C., W.R.J.) and Horticultural Sciences (M.C.D.), Texas A&M University, College Station, Texas 77843

ABSTRACT

The effects of a severe water deficit on total root (L_t) and axial (L_x) hydraulic conductances and on the development of the hypodermis, endodermis, and xylem were studied in sorghum (*Sorghum bicolor* L.). Water deficit was imposed in the upper rooting zone while the lower zones were kept moist. L_t and L_x were based on water flow rates obtained by applying suction to proximal xylem ends of excised roots. The development of the hypodermis, endodermis, and other tissues were examined by staining with fluorescent berberine hemisulfate and phloroglucinol-HCl. The L_t value ($\times 10^{-8}$ meters per second per megapascal) for unstressed control roots was 22.0 and only 5.9 for stressed roots. The low L_t in stressed roots was attributed, in part, to accelerated deposition of lignin and suberin in the hypodermis and endodermis. Calcofluor, an apoplastic tracer that binds to cellulose, was blocked in stressed roots at the lignified and suberized outer tangential walls of the hypodermis but readily penetrated the cortical walls of similar root regions in controls where the casparian band was not developed. L_x per unit root length was about 100 times lower in stressed roots than in controls because of the persistence of late metaxylem cross-walls and the smaller diameter and lower number of conductive protoxylem and early metaxylem vessels.

Resistances in the radial and axial pathways alter rates of water movement through roots and increase the Ψ[2] gradient required to sustain flows necessary to supply transpirational losses. Studies of maize (6), wheat (9), barley (23), and *Agave deserti* (15) using various flow measurement techniques have shown that water uptake or L_p varied along the length of the root. Variations in L_p have been associated closely with suberization of the endodermis (15, 25) and the presence of lateral roots (23). However, it is difficult to ascertain whether the decline in water conductivity that occurs during development of endodermal cells is related entirely to suberin lamellae deposited around the protoplast or to an additional resistance that might be created by lignin deposits in the cell walls. The hypodermis, similar to the endodermis in structure and detected in many angiosperm species (18), could serve as the initial barrier to radial water movement. Radial water movement across these potential barriers could be influenced by the frequency of the plasmodesmata and hydrophilic micropores that may traverse the suberin lamellae of the hypodermis or exodermis (18) and endodermis (22).

Resistance to water flow in the xylem is usually assumed to be negligible in relation to L_p (6). However, recent studies of roots of soybean (11), barley (24) maize (27), and sorghum (30) indicate that xylem cross-walls may persist for a distance of >0.15 m from the root apex, thus reducing L_x. The above studies indicated that L_p should be determined in conjunction with L_x, when possible, because the latter is not always negligible. Both L_p and L_x are dynamic properties that can be influenced by localized environmental conditions (3, 7, 10, 14, 16, 17, 21) that modify root metabolism and, hence, structural development. In the present study, we assessed the influence of water deficit in the upper rooting zone on root L_p and L_x and on the development of the hypodermis, endodermis, and xylem. Such information is essential when determining the ability of roots to take up water and thus function in the water economy and growth processes of the plant when soil is rewetted after a drought period.

MATERIALS AND METHODS

Plant Culture

Caryopses of sorghum (*Sorghum bicolor* L. cv RS610) were germinated on moistened filter paper. On the third day, each seedling was transferred to a polyvinyl chloride tube (1.0 × 0.1 m) containing coarse expanded vermiculite (Grace Horticultural Products, Cambridge, MA). Vermiculite was used as a solid growing medium because it exhibits very little increase in mechanical strength during drying. The upper 0.03 m of the tube was packed with coarse fritted clay (Balcones Mineral Corp., Flatonia, TX) to provide mechanical support for the base of the shoot. Plants were maintained in a growth chamber with 14-h daylength, day/night temperatures of 29/25°C, daytime RH of about 60%, and PPFD of about 500 μmol m^{-2} s^{-1} (measured with Li-Cor LI-190 quan-

[1] Research supported in part by a Rockefeller Foundation grant. Texas Agricultural Experiment Station paper No. 30143.

[2] Abbreviations: Ψ, water potential; L_t, total root hydraulic conductance per unit area of root surface ($m \cdot s^{-1} \cdot MPa^{-1}$); L_p, root radial hydraulic conductivity; L_x, axial hydraulic conductance per root segment ($m^3 \cdot s^{-1} \cdot MPa^{-1}$); R_x, axial hydraulic resistance per unit root length ($m^{-4} \cdot s \cdot MPa$); Ψ_s, osmotic potential; θ_v, volumetric moisture content; J_v, water flow rate; ΔP, pressure difference; EMX, early metaxylem; LMX, late metaxylem; PX, protoxylem; R_r, radial resistance to water flow.

tum sensor) at the canopy level. Plants were irrigated daily with full-strength nutrient solution (4) for 18 d from the date of imbibition and then exposed to water deficit by withholding irrigation for 15 d. Drying in the upper 0.15-m rooting zone was hastened by continuously pumping air through three perforated concentric tubes installed at the 0.15-m depth in the polyvinyl chloride tube.

Growth, Water Status, and Leaf Conductance

The dates when adventitious roots exserted from the crown were recorded, and roots were identified with attached colored threads. Their final lengths were determined at the end of the treatment period, and average root extension rates (mm d^{-1}) were calculated by dividing the final length by the growth period.

At the end of the 15-d stress treatment, roots to be sampled were carefully separated from the vermiculite. Ψ of root segments taken at 0 to 5, 5 to 10, and 10 to 15 mm from the root apex were measured using Wescor C52 thermocouple psychrometers and a H33T microvoltmeter. Ψ_s was determined after freezing and thawing the same samples in liquid nitrogen and assuming negligible dilution by apoplastic water. Pressure potentials were calculated by subtracting Ψ_s from Ψ. Vermiculite moisture contents were determined by a gravimetric method. θ_v was obtained by multiplying the vermiculite moisture content by the bulk density. A moisture release curve for vermiculite was obtained using a pressure plate.

Ψ and Ψ_s for leaves were measured with Wescor C52 thermocouple psychrometers. Leaf conductance was determined with a Li-Cor 1600 steady-state porometer. Leaf extension rates were measured daily with a ruler.

Measurement of L_t and L_x

At the end of the stress treatment, adventitious roots from the fourth or fifth node were exposed by carefully removing the vermiculite and excised. The cortex was carefully removed from around the stele from the proximal 5 mm while the remainder of the root was immersed in aerated 0.10 strength nutrient solution having a temperature of about 22°C. The exposed stele was inserted into a glass microcapillary tube and the junction sealed with a mixture of 95% dehydrated lanolin and 5% paraffin (w/w). With this procedure, axial flow through the cortical apoplast was avoided when suction was applied to the stele (15, 16, 24). The root was left in nutrient solution for about 2 h to exude sap under root pressure and gently remove air bubbles in the xylem. A partial vacuum, as measured with a pressure meter (Vacu/Trol; Spectrum Medical Industries, Los Angeles, CA) was applied to the open end of the microcapillary tube attached to the stele. The rate of water flow from the cut end was determined by recording the time required for the meniscus to move a predetermined distance. L_t and L_x were calculated from measurements of flow rates and pressure gradients. Measurements of L_t were based on the relationship between J_v ($m^3\ s^{-1}$) and applied ΔP (16, 17), according to the equation (16):

$$L_t = \frac{\Delta J_v}{\Delta P} \cdot \frac{1}{A}$$

where A (m^2) is the root surface area obtained by measuring the diameter and the length of the root and L_t is in $m^3 \cdot m^{-2} \cdot s^{-1} \cdot MPa^{-1}$.

L_x per root segment ($m^3 \cdot s^{-1} \cdot MPa^{-1}$) was measured for the same roots immediately following determination of L_t. To obtain the initial measure of L_x, the apical 10-mm segment was excised, and the J_v entering the open xylem ends under suction was determined. Variability in L_x along the root was determined by removing successive segments beginning at the apex and measuring L_x on the remaining segment.

Histochemical Tests and Image Processing

Immediately after L_t and L_x were measured, serial freehand transverse sections were made from the same root. The sections were transferred to multichamber holders and stained with fluorescent berberine hemisulfate and counterstained with aniline blue (to partially quench fluorescence from epidermal and cortical walls) to test for the presence of suberin and lignin (1). Berberine has a higher affinity for cell walls containing bound phenolic components in the form of suberin or lignin than for unmodified walls. Similar sections were stained with phloroglucinol-HCl to test for lignin (8). Adjacent sections from roots with apices that had been perfused with Calcofluor (see procedure for apoplastic tracer below) but not mounted in glycerin were cleared in 1% (w/v) NaOH for 12 h (20) and stained with berberine hemisulfate (1) to detect casparian bands. The use of NaOH was based on a previous observation that the encrusted casparian band suberin was more resistant to alkali digestion than the adcrusted lamellar suberin. A minimum of four roots were sampled for staining. Stained sections were either viewed in white light or in the violet light of a Zeiss II fluorescence microscope and photographed using ASA 100 slide film. A video camera was used to acquire images from the slides. The video signal was used as input into a Zeiss-Kontron SEM image-processing system, and the percentage of cross-sectional cell area that was lignified was determined for the hypodermis and the endodermis. Cortical, pericycle, and xylem cells were also viewed.

Apoplastic Tracers and Test for Conductivity

Calcofluor white M2R (also called Fluorescent Brightener 28), a fluorescent apoplastic tracer that binds to cellulose, was used to estimate potential accessibility of the radial and axial apoplastic pathways of water flow. After L_t was measured, roots with apices were placed in aerated Calcofluor, 0.01% (w/v), a nontoxic level (20), for 2 h, and then the proximal xylem ends were subjected to a 0.04-MPa suction for the following 2 h. Transverse sections were mounted in glycerin, immediately viewed under the epifluorescence microscope, and photographed. The conductive xylem vessels were made visible by perfusing open-ended root segments (sectioned transversely at increasing distances from the root apex), under a 0.04-MPa suction, with 0.01% (w/v) Calcofluor for 15 to 20 min. Root transverse sections were then mounted in glycerin, viewed under the epifluorescence microscope, and photographed. The diameters of the xylem vessels and percentage of the xylem vessels liginifed (based on cross-sectional area) were determined from micrographs using the SEM-image-processing system.

Presence of Cross-Walls

Roots from replicate control and stressed plants were fixed in a solution of formalin, ethyl alcohol, and acetic acid (5:90:5, v/v; ref. 8), dehydrated in an alcohol series, critical point dried with liquid CO_2, placed in sample mounts, and sputter coated with 60% gold and 40% palladium. Longitudinal sections were viewed under the T330A SEM (JEOL) to determine the presence of cross-walls in xylem vessels.

RESULTS

Growth, Water Status, and Leaf Conductance

θ_v of the vermiculite decreased substantially in the upper 0.15-m rooting zone in response to plant water extraction and forced air drying, reaching 6.5% at the end of the 15-d stress treatment. At depths of about 0.40 m and below, θ_v was near 80%. For well-watered controls, θ_v was about 80% at all depths. Based on the moisture release curve for vermiculite, θ_v values of 6.5 and 80% were equivalent to −3.5 and −0.02 MPa, respectively.

Extension rates of stressed roots that developed during the stress period were 8 ± 2 mm d^{-1}, whereas extension rates of controls were 60 ± 8 mm d^{-1}. In the stress treatment, the roots that developed during the stress period were mostly confined to the upper 0.15-m rooting zone and had Ψ values lower than the controls (Fig. 1). However, the roots that were exserted before stress imposition reached the lower, wetter vermiculite, and Ψ values of their apical segments were comparable to the controls. In the apical 5-mm region of stressed roots, desiccation led to a Ψ as low as −3.2 MPa and turgor was close to zero (Fig. 1). In the controls, Ψ and turgor potential in the apical region were −0.96 and 0.75 MPa, respectively. However, turgor maintenance in stressed roots was exhibited by tissues behind the 5-mm apical region at levels comparable to controls. When stressed plants were rewatered, there was no resumption of growth by the root apex, but lateral roots were initiated from the basal portion of the root.

Despite the presence of roots in the wet vermiculite below the 0.15-m depth, leaves showed signs of water deficits. Leaf Ψ values and leaf conductances at the end of the 15-d stress treatment were −1.81 ± 0.31 MPa and 0.031 ± 0.006 cm·s^{-1}, respectively, for the treated plants, and −1.38 ± 0.20 MPa and 0.053 ± 0.008 cm·s^{-1}, respectively, for controls. Leaf extension rates were 2.67 ± 0.19 cm·d^{-1} for the treated plants and 4.33 ± 0.49 cm·d^{-1} for the controls.

Root Hydraulic Conductance

J_v increased in both stressed and unstressed control roots as the applied ΔP increased (Fig. 2), but the increase in J_v was less in stressed roots than in controls. L_t, as calculated using the regression coefficients and root surface area, were 5.9 × 10^{-8} m·s^{-1}·MPa^{-1} for stressed roots and 22.0 × 10^{-8} m·s^{-1}·MPa^{-1} for controls (Table I). These values (expressed as L_t·A) were equivalent to 1.5 × 10^{-11} and 5.5 × 10^{-11} m^3·s^{-1}·MPa^{-1}, respectively, to allow comparison below with L_x values which cannot be normalized with respect to unit surface area of root.

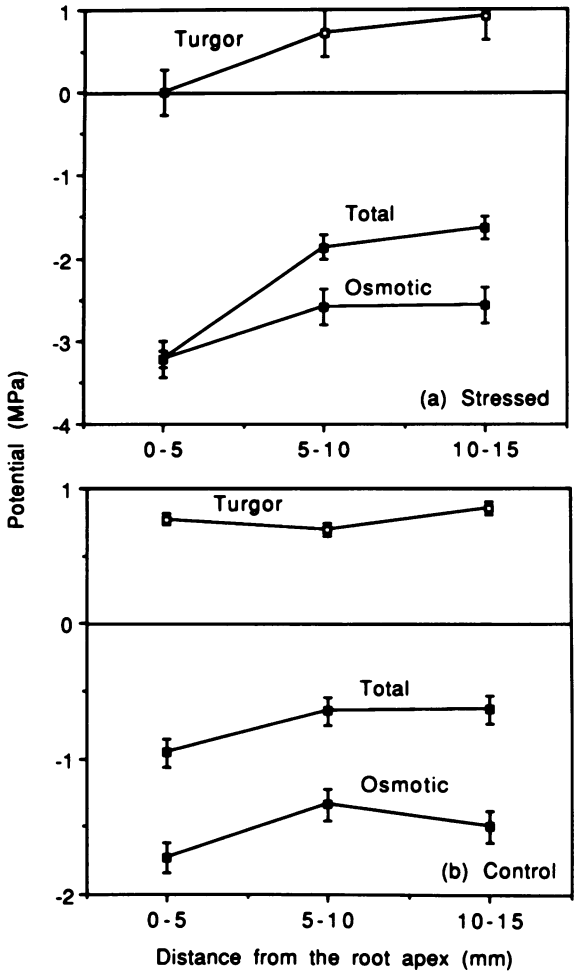

Figure 1. Total Ψ, Ψ_s, and pressure potential of roots as a function of distance from the root apex for stressed (a) and control (b) sorghum roots. Points, means; bars, SE (n = 3).

L_x of control and stressed roots was measured successively on root segments of decreasing lengths (Fig. 3). In control roots, which were longer than those used for L_t measurements, L_x increased as root segments were removed from the apical end (the experimental sequence was from right to left in Fig. 3), because axial flow was through root segments of decreasing length and, therefore, decreasing resistance. For stressed roots, which were shorter because of their slower growth, L_x remained virtually unchanged as segments were removed, suggesting that blockages to axial flow existed throughout the length of the root. When L_x was plotted as a function of $1/l$ (where l is length of remaining open root segment; Fig. 3, inset), the slope ($L_x l$) for controls was 18.3 × 10^{-11} m^4·s^{-1}·MPa^{-1} (R^2 = 0.975) and 0.166 × 10^{-11} m^4·s^{-1}·MPa^{-1} for stressed roots. Expressed as R_x per unit length ($R_x = 1/L_x l$), these values correspond to 5.45 and 600 × 10^9 m^{-4}·s·MPa, respectively.

Root Structure and Movement of Apoplastic Tracers

The developmental stages of endodermal cells previously described for barley (2) were adopted for description of the

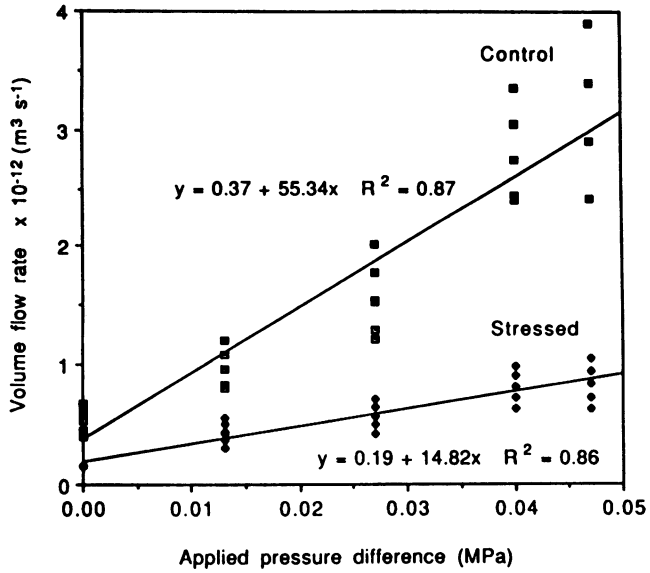

Figure 2. J_v as a function of the applied ΔP for the apical 80 mm of root. Intercepts, regression coefficients, and correlation coefficients for control and stressed roots are presented.

development of the hypodermis and endodermis of sorghum. State I refers to formation of the casparian band, state II includes the casparian band and formation of suberin lamellae around the protoplast, and state III describes the most advanced stage and includes tertiary thickening and lignification.

For stressed roots, results from berberine staining confirmed that at 10 and 70 mm from the apex, the hypodermis and endodermis were both in state III (Fig. 4, a–d). At 3 mm from the root apex, the hypodermis and endodermis were also in state III but not as lignified as the corresponding cells 5 and 10 mm from the apex (not shown). The phloroglucinol-HCl test for lignin confirmed the advanced developmental states of the hypodermis and endodermis of stressed roots (Fig. 4, e and f). Both berberine and pholoroglucinol tests showed that, in the hypodermis of stressed roots (Fig. 4, a, c, and e), the outer tangential walls were more lignified than the radial and inner tangential walls. In the endodermis (Fig. 4, b, d, and f), the inner tangential walls were more lignified than the radial and outer tangential walls. The EMX walls appeared to be lignified to the same extent in the different zones in stressed roots. However, the frequency and degree of lignification of pericycle cells (interior to endodermis) and parenchyma cells located between the LMX increased with distance from the apex (Fig. 4, b, d, and f). Cortical cells adjacent to the hypodermis began to show signs of lignification at distances >70 mm from the root apex (not shown). SEM image analysis of stressed roots indicated that in the hypodermis a greater proportion of the cross-sectional area was occupied by lignified walls than in the endodermis. For example, at 10 and 70 mm from the root apex, about 35 and 40%, respectively, of the cross-sectional cell areas of the hypodermal cells and 20 and 30%, respectively, of the endodermal cell areas were lignified. No comparable lignin deposition was observed at the same locations in controls (Fig. 5, a–d). Even in the more basal portion of control roots 450 mm from the root apex, the hypodermal cells were still in state II (with casparian band and suberin lamellae), whereas the endodermal cells were in state III (Fig. 5, e and f).

An apoplastic barrier at the hypodermis of stressed roots was revealed by perfusion with Calcofluor, an apoplastic fluorescent tracer. The tracer clearly penetrated the epidermal walls but was blocked at the lignified layer in the outer tangential walls of the hypodermis in regions closer to the apex, *i.e.* 3 (not shown) to 10 mm from the apex (Fig. 6a). Wounding the tissue with a needle allowed the tracer to penetrate the cortical walls up to the endodermis (Fig. 6b). The controls, being developmentally younger, allowed Calcofluor penetration into the cortical walls at 3 (not shown), 10 (Fig. 6c), and 50 mm from the apex (not shown). But at 60 to 70 mm from the apex, Calcofluor was blocked at the outer tangential walls of the hypodermis (Fig. 6d). When sections adjacent to the 60- to 70-mm region (previously treated with Calcofluor) were cleared with NaOH and stained with berberine, distinct fluorescence was observed in the casparian band region in the radial walls (not shown). Direct berberine staining of similar sections from control roots also

Table I. *Vessel Diameter, Percentage of EMX Vessel Lignified (Based on SEM Image Analysis on a Cross-Sectional Area), and Percentage of EMX Vessels Conductive to Calcofluor for Stressed and Control Sorghum Roots*

Results are means ± SE. Numbers of replications equal 10 each for diameter and % lignified and equal 3 for conductivity to Calcofluor.

Measurement	Stressed		Control	
	10 mm[a]	70 mm	10 mm	70 mm
Vessel diameter (μm)				
PX	7.4 ± 0.4	6.2 ± 0.2	13.2 ± 0.6	11.7 ± 0.3
EMX	15.0 ± 0.6	14.5 ± 0.6	28.5 ± 1.5	27.3 ± 0.8
LMX	64.0 ± 0.9	75.0 ± 2.3	80.0 ± 1.9	84.0 ± 0.2
% of EMX lignified	52.3 ± 2.6	54.2 ± 2.9	25.5 ± 1.3	32.0 ± 1.1
% of PX and/or EMX conductive to Calcofluor	37.7 ± 3.8	33.3 ± 1.5	95.5 ± 1.9	91.3 ± 2.5

[a] Distance from the root apex.

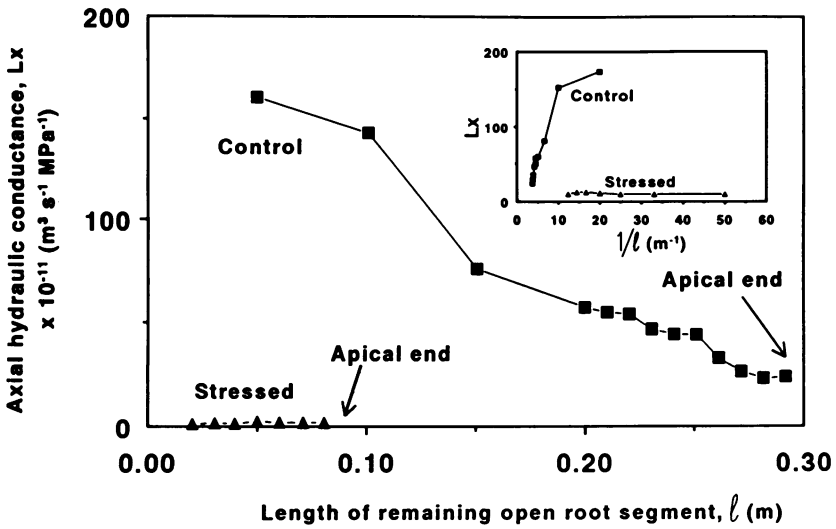

Figure 3. L_x measured with decreasing length of root segment. Conductance values were obtained by excising segments of the root starting from the apical end (arrowheads). Measurements began with segments of 0.3 m for control and 0.09 m for stressed roots (in which the apical 0.01 m had been previously excised) and terminated when only the basal (older) segments remaining were 0.05 m long for the control and 0.02 m for stressed roots. Values are averages of six replications and are expressed per root segment, not per unit length. SE values are within 15% of the mean. Note that stressed roots were shorter because of low axial growth rates. It was assumed that L_p was small in relation to L_x in these open-ended segments.

showed stronger fluorescence in the hypodermal casparian band regions (state I) at 70 mm (Fig. 5c) than at 10 mm from the apex (Fig. 5a). Additional fluorescence at the walls of the hypodermal cells from the 60 (not shown) to 70-mm region (Fig. 5c) indicates that development of the casparian band was immediately followed by deposition of suberin lamellae (state II).

Scanning electron micrographs showed that intact LMX cross-walls were present in some instances in a zone as far as 260 mm behind the root apex in the controls (not shown). LMX cross-walls persisted in the shorter (70–120 mm) but older stressed roots with about four cross-walls per millimeter length of xylem vessel. Perfusion of open-ended root segments with Calcofluor revealed that, in the controls, the PX (Fig. 6e), EMX (Fig. 6f), and LMX (Fig. 6g) were first conductive at 10, 70, and 260 mm from the root apex, respectively. At 260 mm from the apex, most of the LMX vessels were conductive. In the stressed roots, only the EMX vessels were conductive even at 100 mm from the apex (Fig. 6h). Although some EMX vessels were conductive in both treatments (Table I), only about one-third were so in stressed roots, whereas >90% were conductive in controls. The internal diameters of these vessels were nearly halved in stressed roots (Table I; *cf.* Fig. 4, b and d, with Fig. 5, b and d), and a larger percentage of the cross-sectional area was lignified.

DISCUSSION

L_t

L_t obtained for unstressed sorghum roots is within the range of values obtained for other species using hydrostatic gradient techniques on single excised root axes (Table II). In the present study, a lower hydrostatic pressure on the proximal root end was achieved using a partial vacuum, a simple technique that has been used effectively in previous studies (15, 16, 24). Hydraulic conductivities obtained by applying a positive pressure on the distal root end may not always agree with L_t values obtained using a physiologically more relevant suction on the proximal end because of asymmetrical properties of roots or artifacts introduced by high pressures in the pressurizing gas (16, 17, 26). In the present study, L_t was obtained from the linear relation between J_v and applied ΔP shown in Figure 2. The occurrence of J_v even at zero P in Figure 2 has been observed in several studies (5, 13, 16, 17, 29) and was attributed to transport of solutes into the xylem resulting in osmotically driven water influx. The relationship between J_v and ΔP usually becomes linear at higher P values when high J_v values increase the Ψ_s in the xylem because of dilution of solutes, but we did not observe pronounced curvilinearity in our study.

The low L_t we obtained for stressed roots suggests that water flow across the root in the apoplast is decreased, in part at least, by extensive suberization and lignification (state III) of the hypodermis and endodermis (Fig. 4, e and f). That an initial barrier might reside at the outer tangential walls of the hypodermis is supported by the observation that the apoplastic tracer Calcofluor was blocked at that location for most of the length of the stressed root. Here, lignification is likely to increase resistance to water flow, limiting access to the plasma membranes of hypodermal cells. Formation of suberized lamellae in the hypodermis (18) would not itself block the apoplastic pathway provided by the primary cell wall, but the casparian band-like structure is believed to behave as an apoplastic barrier in the hypodermis (18, 19) analogously to its role in the endodermis. The significantly lower L_t in stressed roots suggests that there is a high resistance apoplastic pathway in the suberized and lignified root regions, presumably composed of small hydrophilic micropores of low conductivity.

In unstressed controls, Calcofluor clearly penetrated the epidermal walls but was blocked at the outer tangential walls of the hypodermis (Fig. 6d) in regions where developed casparian bands were observed by berberine staining (Fig. 5c). In species such as barley that do not have a suberized hypodermis (2), a reduction in L_t coincides with suberization and subsequent lignification of the endodermis during its normal development. This has led to the idea that part of the radial water flow in the root is symplastic, and unaffected by the

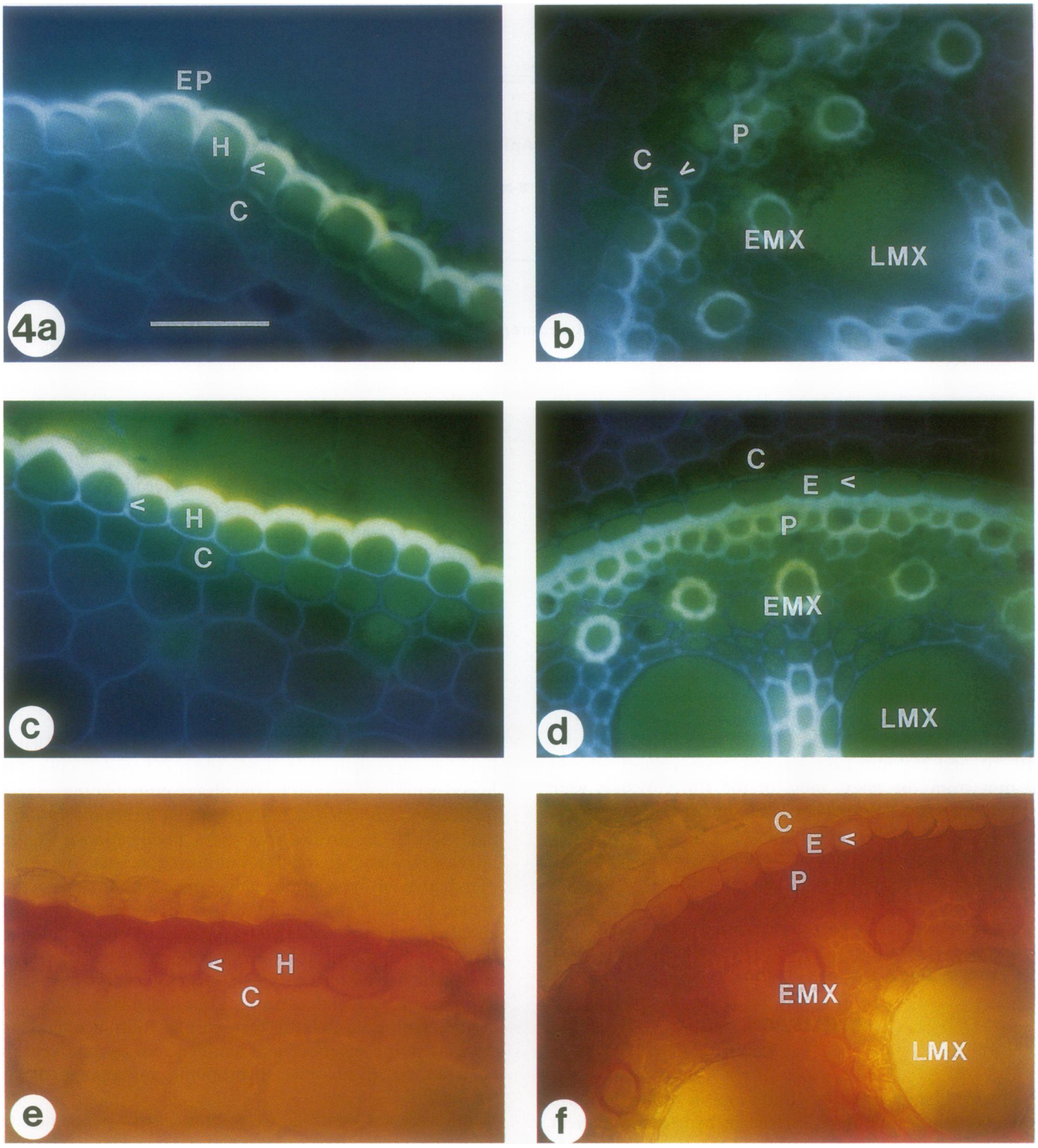

Figure 4. Fresh cross-sections of stressed sorghum root (×500) stained with berberine hemisulfate (a–d) and phloroglucinol-HCl (e and f) and viewed with epifluorescence and white light optics, respectively. a and b, Ten millimeters from root apex; c to f, 70 mm from root apex. EP, Epidermis; H, hypodermis; C, cortex; E, endodermis; P, pericycle. Arrowhead, Location of casparian band on one side of radial wall. Note distinct lignification on the outer tangential walls of the hypodermis and on the inner tangential walls of the endodermis. Bar = 50 μm.

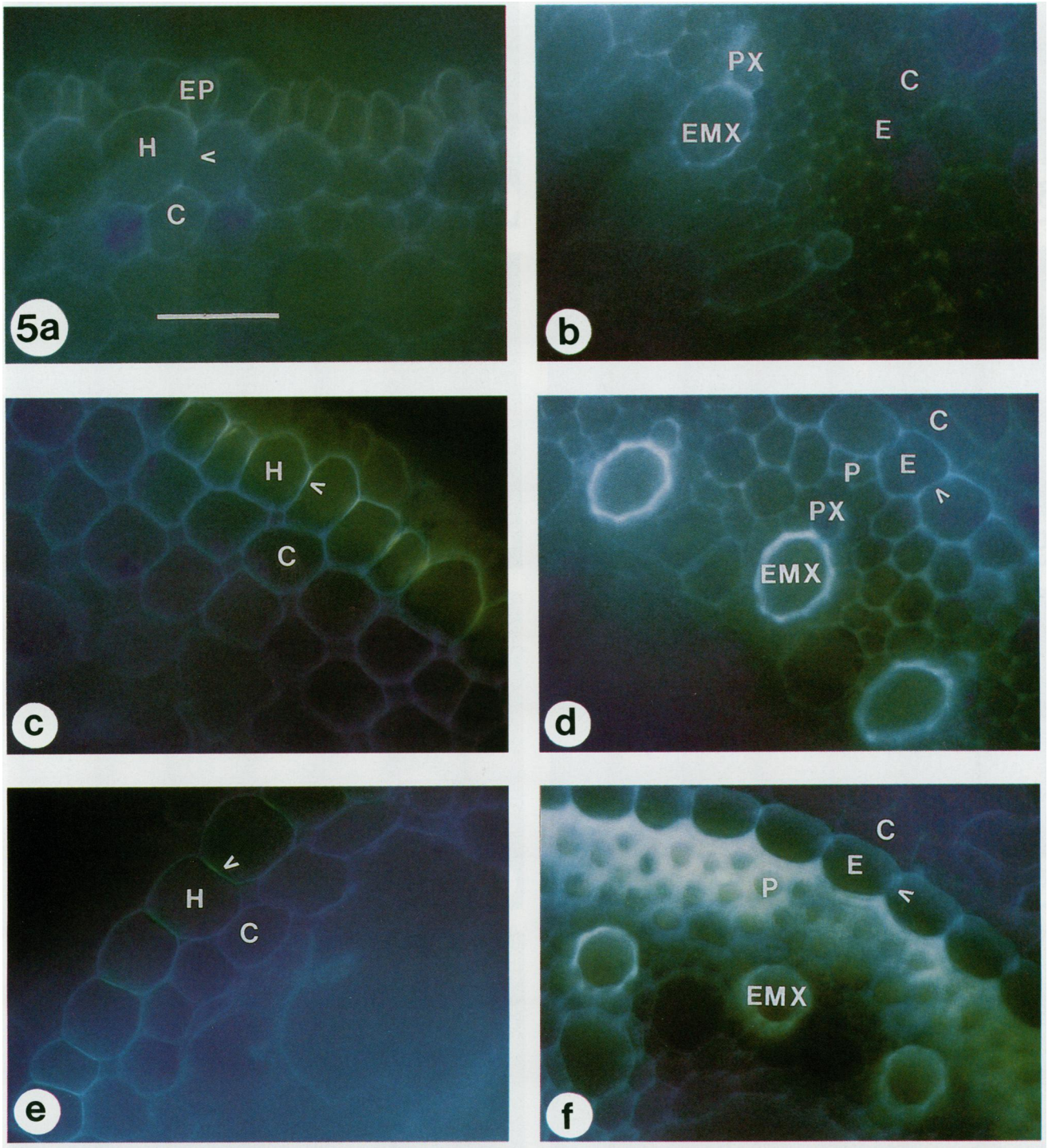

Figure 5. Fresh cross-sections of unstressed sorghum root (×500) stained with berberine hemisulfate and viewed with epifluorescence optics (a–f). a and b, Ten millimeters from root apex; c and d, 70 mm from root apex; e and f, 450 mm from root apex. EP, Epidermis; H, hypodermis; C, cortex; E, endodermis; P, pericycle. Arrowhead, Location of casparian band on one side of radial wall. Bar = 50 μm.

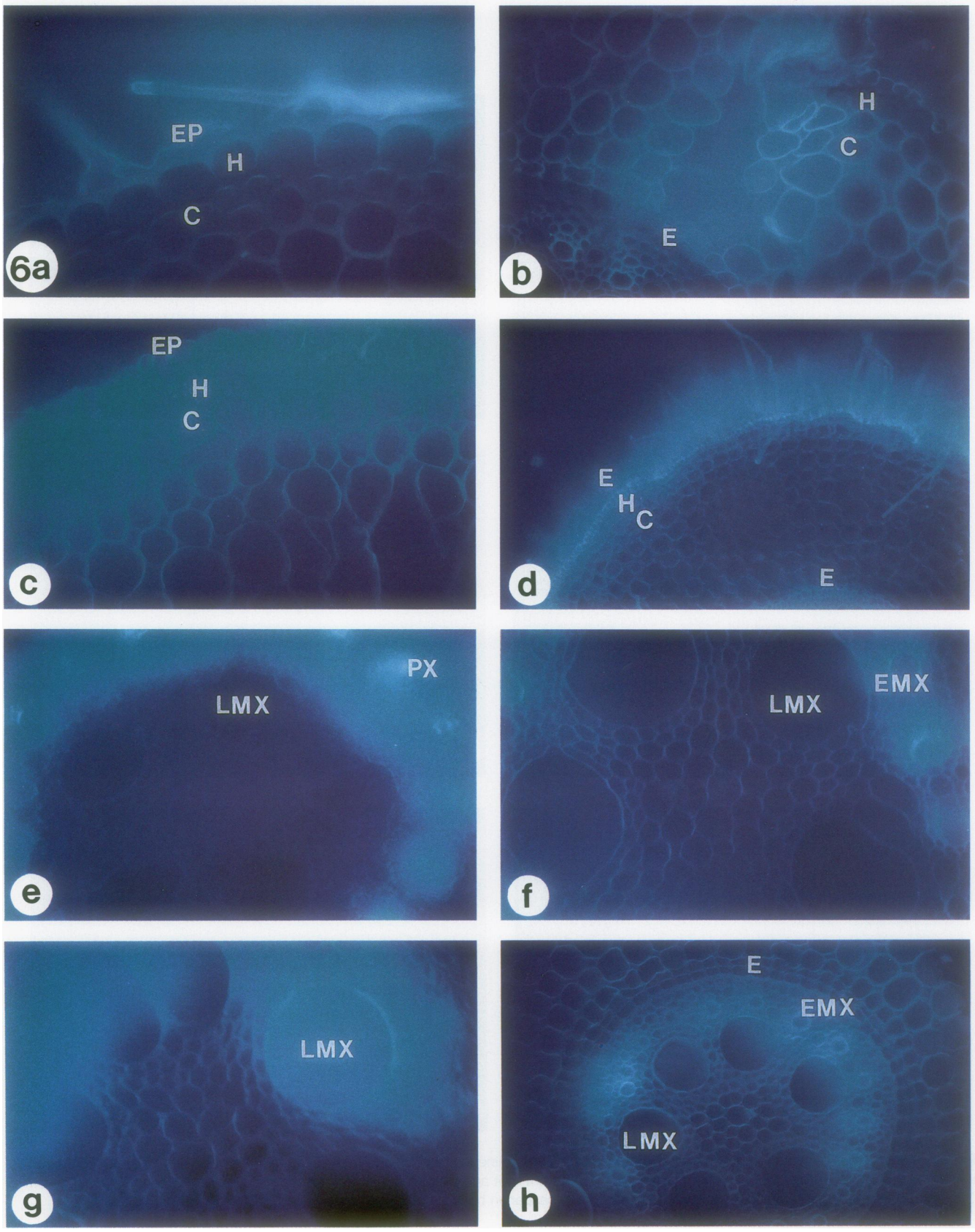
EP
H
C
6a
H
C
E
b
EP
H
C
c
E
H
C
E
d
PX
LMX
e
EMX
LMX
f
LMX
g
E
EMX
LMX
h

development of the endodermis, and that part is apoplastic as far as the endodermis (2). By analogy, similar constraints could apply to the flow of water across the hypodermis during its suberization and lignification. However, although the frequency of the plasmodesmata in endodermal tangential walls is known to be high (2), there are relatively few estimates for the hypodermis. Thus, in the present study, it is not possible to unambiguously separate the effects of hypodermal and endodermal development on the marked decrease in L_t in stressed roots.

L_x

L_x was substantially lower in stressed roots as compared with the controls (Fig. 3), presumably because of the persistence of LMX cross-walls and the smaller diameter of the PX and EMX vessels (Table I). However, we do not know the frequency of PX and EMX cross-walls along the root. These cross-walls in some way may have kept L_x low even though roots became shorter (Fig. 3). In unstressed maize and sorghum, the seminal and nodal roots commonly reached lengths of 300 mm before the LMX cross-walls broke down (30). With age, cross-walls disappeared, and the LMX became conductive (this study). In stressed roots, however, the disappearance of cross-walls appears to be sensitive to water deficit. We observed cross-walls persistent even in relatively mature zones (14–15 d old) or in zones of an age similar to unstressed controls in which most of the LMX vessels were conductive.

The Poiseuille equation is commonly used to calculate L_x, but one must take into account the variation in the number and conductivity of the xylem vessels in stressed and unstressed roots to obtain reliable estimates. In maize (6), calculated values of L_x were larger than measured by a factor of 2 to 5, presumably due to assumptions concerning viscous flow in an ideal cylindrical vessel and uncertainty as to which xylem elements were conductive.

In many earlier estimates (29) of root L_p, it has been assumed that L_x was high relative to L_p, but in the present study with stressed roots, that may not be the case. The effect of an appreciable axial resistance would be to attenuate the lowered xylem Ψ so that at increasing distance along the root the hydraulic component to the driving force on water movement (both radially and axially) is less than applied to the base of the root (6). It is instructive to compare resistances to water flow in sorghum with those in maize (6). In maize, R_r was 4×10^6 $m^{-1} \cdot s \cdot MPa$ and R_x was 19×10^9 $m^{-4} \cdot s \cdot MPa$ for root segments in excess of 30 mm from the tip. In the tip segment, R_x increased greatly to $>10{,}000 \times 10^9$ $m^{-4} \cdot s \cdot MPa$. In our study, the corresponding values for controls (using $1/L_t$ as a first approximation) were $R_r = 4.54 \times 10^6$ and $R_x = 5.45 \times 10^9$. Thus, ignoring the tip zone, sorghum roots had about one-third the resistance to axial flow of water, whereas the total resistance of sorghum was very similar to the R_r in maize. The significance of R_x and R_r to water flow can be estimated from the parameter α, where $\alpha^2 = 2\pi a\, R_x/R_r$, and a is root diameter. In maize (6), α along most of the root was 4.5, whereas in the present study of sorghum, it was 1.9 in controls and 21.7 in stressed roots. From Figure 6 in ref. 6, the calculated effect of α on Ψ_x in controls would be negligible, so that L_p would largely determine L_t, except for the tip zone. However, in stressed roots, the effect of α would be to greatly diminish the driving force on water movement, so that L_t would not provide an acceptable estimate of L_p. This suggests that, in stressed roots, changes in L_t cannot be attributed solely to a change in the R_r.

Table II. *Root Hydraulic Conductance from Different Plant Species*[a]

Plant	$L_t \times 10^{-8}$ m s^{-1} MPa^{-1}	Technique	Ref.
Sorghum			
Stressed	5.9[b]	Low hydrostatic pressure to proximal root end	Present study
Control	22[b]	Low hydrostatic pressure to proximal root end	Present study
Maize	1–5	Osmotic gradient, root pressure probe[c]	6
	20–25	Hydrostatic gradient, root pressure probe[c]	
Wheat	1.6–5.5	Osmotic gradient[c]	9
Maize	0.9–4.8	Osmotic gradient[c]	
Agave	23	Low hydrostatic pressure to proximal root end	16

[a] Expressed as root hydraulic conductivity in refs. 6, 9, and 16. [b] L_t calculated using the regression coefficients in Figure 2 of this study. [c] Procedure did not indicate how cortical flow was prevented.

Significance of Changes in Root Structure to Water Relations of the Plant

We have shown that a severe water stress in the upper portion of the rooting medium significantly decreased axial growth of adventitious roots that were initiated during the stress treatment. It also induced lignification and suberization closer to the root apex. The tolerance of roots to severe water

Figure 6. Fresh cross-sections from stressed (a and b) and control (c and d) sorghum root segments (with apices) treated with 0.01% aerated Calcofluor white M2R (2 h immersion, then 2 h immersion + 40 kPa suction on proximal end). a, Stressed, 10 mm from root apex, ×500; b, stressed, wounded 10 mm from root apex, ×500; c and d, control, 10 and 70 mm from root apex, respectively. Cross-sections from control (e, 10 mm from apex, ×400; f, 70 mm from apex, ×400; g, 260 mm from apex, ×500) and stressed (h, 100 mm from apex, ×200) segments after perfusing open-ended root segments with Calcofluor for 20 min under 40 kPa suction. All sections were viewed under epifluorescence optics. EP, Epidermis; H, hypodermis; C, cortex; E, endodermis.

deficits may be increased by changes such as ligno-suberization, which in turn could restrict the loss of liquid water and water vapor to the surrounding medium. Accelerated lignification and suberization will probably involve activation of peroxidases (12, 28) or their *de novo* synthesis induced by low Ψ. We have shown that lignification of the hypodermis, endodermis (Fig. 4), xylem vessels and the meristematic pericycle cells (Fig. 4, b, d, and f). Such modifications by helping conserve water internally could have contributed to bulk turgor maintainance in the basal root regions (Fig. 1a) and to some degree retained the capability of those regions to produce lateral roots during 2 to 3 d of rewetting. When lateral roots develop, they break through the endodermal and hypodermal barriers and possibly decrease the resistance to water movement. Apoplastic fluorescent tracers were able to move through the endodermis at the site of secondary root formation in maize and broad bean (19). If the formation of lateral roots transiently decreases the resistance to water movement in the radial pathway, it would be interesting to know whether L_t continues to be limited by the conductivity of xylem vessels with persistent cross-walls.

ACKNOWLEDGMENTS

We thank Dr. Keith Schertz for the use of the epifluorescence microscope and Dr. Fred Miller for supplying the sorghum seeds.

LITERATURE CITED

1. **Brundrett MC, Enstone DE, Peterson CA** (1988) A berberine-aniline blue fluorescent staining procedure for suberin, lignin, and callose in plant tissue. Protoplasma **46:** 133–142
2. **Clarkson DT, Robards AW** (1975) The endodermis, its structural development and physiological role. *In* JC Torrey, DT Clarkson, eds, The Development and Function of Roots. Academic Press, London, United Kingdom, pp 415–436
3. **Drew MC** (1987) Function of root tissues in nutrient and water transport. *In* PJ Gregory, JV Lake, DA Rose, eds, Root Development and Function. Cambridge University Press, Cambridge, United Kingdom, pp 53–70
4. **Drew MC, He CJ, Morgan PW** (1989) Decreased ethylene biosynthesis, and induction of aerenchyma, by nitrogen- or phosphate-starvation in adventitious roots of *Zea mays* L. Plant Physiol **91:** 266–271
5. **Fiscus EL** (1975) The interaction between osmotic and pressure induced water flow in plant roots. Plant Physiol **55:** 917–922
6. **Frensch J, Steudle E** (1989) Axial and radial hydraulic resistance to roots of maize (*Zea mays* L.). Plant Physiol **91:** 719–726
7. **Huang BR, Taylor HM, McMichael BL** (1991) Effects of temperature on the development of metaxylem in primary wheat roots and its hydraulic consequence. Ann Bot **67:** 163–166
8. **Jensen WA** (1962) Botanical Histochemistry. WH Freeman, San Francisco, CA
9. **Jones H, Leigh RA, Wyn Jones RG, Tomos AD** (1988) The integration of whole-root and cellular hydraulic conductivities in cereal roots. Planta **174:** 1–7
10. **Jordan WR, Miller FR** (1980) Genetic variability in sorghum root systems: implications for drought tolerance. *In* NC Turner, PJ Kramer, eds, Adaptation of Plants to Water and High Temperature Stress. Wesley, NY, pp 383–399
11. **Kevekordes KG, McCully ME, Canny MJ** (1988) Late maturation of large metaxylem vessels in soybean roots: significance for water and nutrient supply to the shoot. Ann Bot **62:** 105–111
12. **Kolattukudy PE** (1984) Biochemistry and function of cutin and suberin. Can J Bot **62:** 2918–2933
13. **Kramer PJ** (1983) Water Relations of Plants. Academic Press, Orlando, FL
14. **Moreshet S, Huck MG** (1991) Dynamics of water permeability. *In* Y Waisel, A Eshel, U Kafkafi, eds, Plant Roots—The Hidden Half. Marcel Dekker, Inc., New York, pp 605–626
15. **Nobel PS, Sanderson J** (1984) Rectifier-like activities of roots of two desert succulents. J Exp Bot **35:** 727–737
16. **Nobel PS, Schulte PJ, North GB** (1990) Water influx characteristics and hydraulic conductivity for roots of *Agave deserti* Engelm. J Exp Bot **41:** 409–415
17. **Passioura JB** (1988) Water transport in and to roots. Annu Rev Plant Physiol Mol Biol **39:** 245–265
18. **Peterson CA** (1988) Exodermal casparian bands. Their significance for ion uptake by roots. Physiol Plant **72:** 204–208
19. **Peterson CA, Emanuel ME, Humphreys GB** (1981) Pathway of movement of apoplastic fluorescent dye tracers through the endodermis at the site of secondary root formation in corn (*Zea mays*) and broad bean (*Vicia faba*). Can J Bot **59:** 618–625
20. **Peterson CA, Perumalla CJ** (1984) Development of the hypodermal casparian band in corn and onion roots. J Exp Bot **35:** 51–57
21. **Richards RA** (1987) Physiology and breeding of winter-grown cereals for dry areas. *In* JP Srivastava, E Porceddu, E Acevedo, S Verma, eds, Drought Tolerance in Winter Cereals. John Wiley and Sons Ltd., Chichester, United Kingdom, pp 133–150
22. **Robards AW, Clarkson DT, Sanderson J** (1979) Structure and permeability of the epidermal/hypodermal layers of the sand sedge (*Carex arenaria* L.) Protoplasma **101:** 331–347
23. **Sanderson J** (1983) Water uptake by different regions of the barley root. Pathways of radial flow in relation to development of the endodermis. J Exp Bot **34:** 40–53
24. **Sanderson J, Whitebread FC, Clarkson DT** (1988) Persistent xylem cross-walls reduce axial hydraulic conductivity in the apical 20 cm of barley seminal root axes: implications for the driving force for water movement. Plant Cell Environ **11:** 247–256
25. **Sands R, Fiscus EL, Reid CPP** (1982) Hydraulic properties of pine and bean roots with varying degrees of suberization, vascular differentiation and mycorrhizal infection. Aust J Plant Physol **9:** 556–559
26. **Shone MGT, Clarkson DT** (1988) Rectification of radial water flow in the hypodermis of nodal roots of *Zea mays.* Plant Soil **111:** 223–229
27. **St Aubin G, Canny MJ, McCully ME** (1986) Living vessel elements in the late metaxylem of sheathed maize roots. Ann Bot **58:** 577–588
28. **Varner JE, Liang-Shiou Lin** (1989) Plant cell wall architecture. Cell **56:** 231–239
29. **Weatherley PE** (1982) Water uptake and flow in roots. *In* OL Lange, PS Nobel, CB Osmond, H Ziegler, eds, Encyclopedia of Plant Physiology, Vol 12B. Springer-Verlag, Berlin, Germany, pp 79–109
30. **Wenzel CL, McCully ME, Canny MJ** (1989) Development of water conducting capacity in the root systems of young plants of corn and some other C_4 grasses. Plant Physiol **89:** 1094–1101